Early-life origin of prostate cancer through deregulation of miR-206 networks in maternally malnourished offspring rats

Luiz Portela
Sao Paulo State University Julio de Mesquita Filho: Universidade Estadual Paulista Julio de Mesquita Filho
Flavia Constantino
Sao Paulo State University Julio de Mesquita Filho: Universidade Estadual Paulista Julio de Mesquita Filho
Ana Camargo
Sao Paulo State University Julio de Mesquita Filho: Universidade Estadual Paulista Julio de Mesquita Filho
Sergio Santos
Sao Paulo State University Julio de Mesquita Filho: Universidade Estadual Paulista Julio de Mesquita Filho
Ketlin Colombelli
Sao Paulo State University Julio de Mesquita Filho: Universidade Estadual Paulista Julio de Mesquita Filho
Matheus Fioretto
Sao Paulo State University Julio de Mesquita Filho: Universidade Estadual Paulista Julio de Mesquita Filho
Luisa Barata
Sao Paulo State University Julio de Mesquita Filho: Universidade Estadual Paulista Julio de Mesquita Filho
Erick Ramos
Sao Paulo State University Julio de Mesquita Filho: Universidade Estadual Paulista Julio de Mesquita Filho
Wellerson Scarano
Sao Paulo State University Julio de Mesquita Filho: Universidade Estadual Paulista Julio de Mesquita Filho
Carlos Moreno
Emory University School of Medicine
Luis A Justulin (l.justulin@unesp.br)

Sao Paulo State University Julio de Mesquita Filho: Universidade Estadual Paulista Julio de Mesquita Filho https://orcid.org/0000-0001-6142-3515

Research Article

Keywords: DOHaD, prostate, maternal low protein diet, steroidogenesis, miRNAs

Posted Date: April 18th, 2022

DOI: https://doi.org/10.21203/rs.3.rs-1546693/v1

Abstract

The Developmental Origins of Health and Disease (DOHaD) has provided the framework to assess how early life experiences can shape health and disease throughout the life course. While maternal malnutrition has been proposed as a risk factor for the developmental programming of prostate cancer (PCa), the molecular mechanisms remain poorly understood. Here, we found an association between deregulation of steroidogenesis and impairment of the ventral prostate (VP) growth in young offspring rats exposed to maternal low protein diet (LPD) during gestation and lactation. Reanalysis of RNA-seq data demonstrated that miR-206 was upregulated in the VP of young maternally malnourished offspring. Target prediction and in vitro studies identified Plasminogen (PLG) as a direct target of miR-206. To give further insights into the participation of the miR-206-PLG network in prostate carcinogenesis in the progeny submitted to maternal LPD. RT-qPCR analysis revealed deregulation of the miR-206-PLG network in the VP of older rats that developed prostate carcinoma in situ. Furthermore, mimic studies revealed a negative correlation between miR-206 and estrogen receptor α (ESR1) expression in PNT2 cells. Together, we demonstrate that early life estrogenization associated with deregulation of miR-206-networks can contribute to the developmental origins of PCa in maternally malnourished offspring. Understanding the molecular mechanisms by which early life malnutrition affects offspring health can encourage the adoption of a governmental policy for the prevention of non-communicable chronic diseases related to the DOHaD concept.

1. Introduction

Non-communicable chronic diseases (NCDs) are reaching epidemic proportions worldwide, with 41 million deaths each year. The most deadly NCDs are related to cardiovascular diseases, followed by several types of cancers, respiratory tract diseases, and diabetes. Almost 80% of these deaths occur in low- and middle-income countries [1]. Although NCDs are diagnosed mainly in adults, a growing body of evidence strongly supports that exposure to adverse conditions during the formative periods disrupts normal developmental biology and predisposes individuals to high-risk NCDs across the life span. The reprogramming of physiologic intrauterine/early postnatal development forms the basis of the Developmental Origins of Health and Disease (DOHaD) concept [2, 3].

The DOHaD concept has emerged over the past 50 years from the outstanding epidemiologic observations of Barker and Osmond (1986) that poor nutrition early in life was associated with increased infant mortality and ischaemic heart disease in adults in England and Wales [4]. Nowadays, a broad range of epidemiological and experimental studies have confirmed and extended Barker's observations, consolidating gene-environment interactions during early life as a critical risk factor for the increased incidence of NCDs later in life. Although the initial focus of DOHaD studies has been directed to obesity, diabetes, and cardiovascular disease, exposures to environmental stressors have been considered a important risk factor for the developmental origins of several malignancies, including breast and prostate cancers [5–8]. The first author to propose the prenatal origin of prostate cancer (PCa) was William Gardner in 1995, who states that "*The origins of prostatic diseases, including carcinoma, are to be found*

in the in utero influences upon the developing prostate" [6]. Later, Keinan-Boker et al. (2009) demonstrated an increased risk of PCa in Jewish men exposed early in life to famine and stress during the Holocaust. Although tragic, this event allowed researchers to explore the potential association between early-life exposure to stress conditions and increased risk for PCa with aging [7].

In the last decade, clinical and experimental studies have provided significant insights into the molecular mechanisms involved in the developmental origins of PCa. In this regard, intrauterine and early postnatal exposure to estrogens or estrogenic compounds, including endocrine-disrupting chemicals (such as bisphenols and phthalates), have been proven to interfere with prostate developmental biology and the susceptibility of prostatic diseases with aging in both humans [5, 9, 10] and rodent models [11–14]. As such, steroidogenesis deregulation induced by maternal malnutrition has been associated with impairment of prostate growth in young rats [15–20] and higher risk of PCa with aging [21–23].

Accumulating data have suggested modifications in epigenetic markers as the main mechanistic framework explaining how malnutrition during early life impacts offspring health [3, 24]. However, the role of maternal malnutrition on the deregulation of microRNAs-mRNAs networks during prostate development with long-lasting consequences for carcinogenesis has not yet been evaluated. We hypothesize that maternal malnutrition during pregnancy and lactation changes the offspring's steroidogenic profiles parallel with the deregulation of miRNA-mRNA networks during prostate development, thereby creating fertile soil for slow-growing PCa with aging. To address this hypothesis, we used a rat model of maternal malnutrition to evaluate changes in the steroidogenic pathway and the deregulation of key mRNA-miRNA networks potentially involved in the developmental origin of prostate cancer in older offspring rats.

2. Materials And Methods

2.1 Animals and diets

Naive adult (90 days age) females (n = 30) and males (n = 10) Sprague Dawley rats were used. The animals were kept under a controlled temperature (22–25°C), relative humidity (55%), and a photoperiod (12h/12h), with free access to water and food. Breeding proceeded overnight in a harem configuration (1 male to 3 females). After determination of pregnancy through detection of spermatozoa in the vaginal smear (considered gestational Day 1 - GD1), pregnant rats were distributed in Control group (CTR, n = 15): Pregnants rats fed with a normal protein diet (17% protein) during the gestation and lactation; and Gestational and Lactational Low Protein group (GLLP, n = 15): Pregnants rats fed with a low protein diet (6% protein) during the same periods. The diets followed the AIN-93 standards described by Reeves et al. (1993) and were provided by PragSoluções (PragSoluções, SP, Brazil) [25]. The diets were previously used in other studies [15, 21–23].

Litters were reduced to eight pups (four males and four females) on a postnatal day (PND) 1 to maximize lactation performance [26]. Maternal body weight and food intake were recorded every 3rd day until GD

21. Dam and offspring biometric parameters were measured until the end of the experiment. One male offspring (21 days old) from each litter was euthanized by an overdose of ketamine and xylazine, followed by decapitation. Blood and ventral prostate (VP) were collected and processed as described below. The procedures were approved by the Biosciences Institute/UNESP Ethics Committee for Animal Experimentation (Protocol #1178).

2.2 Serum blood hormonal analysis

Blood samples from male offspring (n = 8/group) were centrifuged (2400 g for 20 min), and sera were used to quantify total cholesterol (Labtest®, R76-2/100, Brazil, sensitivity: 0.06 mg/dL), pregnenolone (LifeSpanBioSciences®, LS-F39295, USA, sensitivity: 9.375 pg/mL); dehydroepiandrosterone (DHEA) (Monobind®, CA 7425 – 300, USA, sensitivity: 0.10 ng/mL), estrogen (17βestradiol, Monobind®, CA 4925 – 300, USA, sensitivity: 8.2 pg/mL) and testosterone (17β-hydroxy-4-androstene-3-one, Monobind®, CA 3725-300A, USA, sensitivity: 0.038 ng/mL). The hormonal quantifications were made in 96-well plates using the ELISA plate reader (Epoch™, Biotek Instruments, VT, USA) following the manufacturer's protocol.

2.3 Morphology analysis and gelatin-zymography analyses

Samples of VP lobes from CTR and GLLP groups (n = 6/group) on PND 21 were processed for histological analysis as described by Santos et al. (2019). The slides (5μm) were stained with Hematoxylin/Eosin or with picro sirius red. The slides were analyzed using using the image analyzer Leica Q-win software (Version 3 for Windows) coupled a Leica DMLB 80 microscope. The collagen fiber volume was determined by a red color automatic detection in 10 different microscopic fields (200X) from 6 different VP lobe sections. The collagen volume was shown as a percentage of red-stained areas per total prostatic area.

The gelatin zymography was performed as described in Justulin et al., (2010) [27]. Briefly, frozen VP lobes (n = 6/group) were homogenized in extraction buffer (50 mM of Tris buffer pH 7.5 plus 0.25% Triton-X 100), centrifuged, and the total proteins were quantified by the Bradford method [28]. Aliquots (28 μg protein) were subjected to electrophoresis in 0.1% gelatin-containing polyacrylamide gels (8% acrylamide) in a Bio-Rad MiniProtean II system (Bio-Rad Laboratories Inc., Richmond, CA, USA). Next, the gels were shaken with 2.5% Triton-X100 and incubated overnight in 50 mM Tris-HCl (pH 8.4) containing 5 mM $CaCl_2$ and 1μM $ZnCl_2$ at 37°C. Then, the gels were stained with Coomassie Blue, and areas of proteolysis were measured using ImageJ software (National Institutes of Health). The results were expressed in fold change as the mean ± SD.

2.4 Identification of deregulated miRNAs-mRNAs networks in offspring VP

To identify the potential deregulation in miRNAs-mRNAs networks in the VP of young rats, we reanalyzed data of next-generation sequencing (NGS) from the CTR (n = 4) and GLLP (n = 3) groups. These data were generated by our research group and were available for download at the Gene Expression Omnibus (GEO) database under accession numbers GSE180674 (miRNA) and GSE180673 (mRNA). After, the

differentially expressed (DE) miRNAs and mRNAs were identified using the DESeq2 package (https://bioconductor.org/packages/DESeq2/)[29]. The cut-off significance for miRNA and mRNA was p-value < 0.05 and Log_2 Fold Change ≥ |+0.66≤|-0.66|. After identifying deregulated miRNAs in the rat VP, the predicted target mRNAs were identified using miRWalk 3.0 platform (http://mirwalk.umm.uni-heidelberg.de/) for *Rattus norvegicus* [30]. The cut-off criterion for significance was p-value < 0.05. To further identify the deregulated miRNAs-mRNAs network potentially involved with prostatic disorders, the list of predicted mRNAs was integrated with the DE mRNAs identified in our transcriptome dataset, considering miRNAs upregulated and mRNA downregulated and vice versa.

2.5 Identification of miRNAs commonly deregulated in the offspring VP and human PCa

To identify DE miRNAs in patients with PCa, we explored the Prostate Adenocarcinoma (PRAD-TCGA, https://portal.gdc.cancer.gov/projects/TCGA-PRAD) dataset, with data from 550 samples (52 normal samples and 498 tumor samples). The differentially expressed (DE) miRNAs were identified using the DESeq package[29]. The cut-off significance for both miRNA and mRNA were p-value < 0.05 and Log_2 Fold Change ≥ |+0.66≤|-0.66|. Then, we compared the common DE miRNAs in the VP of maternally malnourished offspring with those from patients with PCa.

2.6 Criteria for selection of miRNA commonly deregulated in the offspring VP and human PCa

To select a miRNA commonly deregulated between VP and human PCa for further analysis, we take into account the higher fold change observed in our RNAseq dataset, the miRNA conservation sequences between *Rattus norvegicus* and human (checked through the miRBase database, http://www.mirbase.org/) [31, 32], and its role on prostate biology [33, 34].

2.7 Identification of selected miRNA-mRNAs networks on human PCa: in silico approach

To further explore the role of selected miRNA-mRNAs networks on PCa, the mRNAs predicted to be regulated by the selected miRNA were subjected to enrichment analysis of molecular pathways, biological processes, and cellular components using the Enrichr tool (https://maayanlab.cloud/Enrichr/) [35, 36]. Subsequently, these mRNAs were applied in overall survival analysis and risk assessment in PCa patients using the SurvExpress platform (http://bioinformatica.mty.itesm.mx:8080/Biomatec/SurvivaX.jsp) [37]. The Human Protein Atlas (HPA) (https://www.proteinatlas.org/) database was used to demonstrate the immunolocalization of deregulated mRNAs in human prostatic samples [38–40].

2.8 Functional validation of selected miRNA in transfected prostatic cell line

The benign prostate cell line (PNT-2, Cell Bank of Rio de Janeiro, Brazil) was cultured using RPMI 1640 medium supplemented with 2 mM L-glutamine, 10% FBS, 50 µg/mL penicillin-streptomycin, and 0.5 µg/mL amphotericin B (GIBCO/Invitrogen). The cells were grown at 37ºC with 5% CO_2 in a humid atmosphere and used up to passage 20. The culture medium was changed twice a week, and throughout the experimental period, the cells were monitored with an inverted microscope (Zeiss Axiovert). For passage, the cells were released with 0.25% trypsin (GIBCO/Invitrogen) for 5 min at 37°C, resuspended in a fresh medium, and plated again. Based on the significance of enriched terms ($p < 0.05$) and its relevance for prostate biology, mRNA was selected for validation through RT-qPCR.

2.8.1 miRNA transfection and Cell Viability Assays

Before transfecting, the specific miRNA mimic (mirVanaTM miRNA Mimic, code: 4464066; MC10409, Thermo Fisher, USA) and its control group formed a complex with the Opti-MEM reduced serum medium (Thermo Fisher Scientific, USA). The PNT-2 cells (8×10^4) were plated in 12-well plates in 800µl of complete RPMI medium per well. Once cells became 80% confluent, transfections were performed using RNAiMAX lipofectamine (Thermo Fisher Scientific, USA) with or without 10 nM of specific miRNA mimic for 16 h at 37^{o}C and 5% CO_2. After 24, 48, and 72 h, cell viability was determined by the MTT reduction method according to the manufacturer's instructions (Sigma-Aldrich)[41, 42]. As absorbance is proportional to cell viability, the percentage of cell viability relative to control cells was quantified in a spectrophotometer (ASYS HITECH GmbH, AUT) using a 96-well plate at 550 nm absorbance.

2.8.2 Wound healing assay

PNT2 cells were cultured in a 6 well plate using RPMI 1640 medium at 37°C and 5% CO2 until they reached 80–100% confluence. After, a 200-µl plastic tip was used to perform a single-line scratch at the highest diameter in all replicates. Cell debris was removed using two PBS washes, and 1,2 mL RPMI supplemented with 10% FBS was added to each well. The analysis of the wound open area was performed at 0, 24, 48, and 72 h, and the results were expressed as a percentage of wound healing, following the equation: % wound healing = [100 − (wound area at Tnh/wound area at T0h)] × 100, where T0h is the time point immediately after the scratch [43].

2.8.3 In vitro validation of selected miRNA and its predicted targets

Total mRNA of PNT2 cells in all treatments was extracted with TRIzol (Thermo Fisher Scientific, USA) as recommended by the manufacturer. Aliquots of 2 µg of total RNA were reverse transcribed using the High-Capacity Kit RNA-to-cDNA (Life Technologies) in a 10-µl reaction according to the manufacturer's instructions. Aliquots of cDNA from each sample were added to a mix of reagents containing primers "sense" and "anti-sense," and the volume was completed to 10 µl with ultrapure water. Primers were designed specifically for target genes after *in silico* filtering. The values obtained for all samples were normalized by the ratio between the target genes and the reference genes (*ACTIN* and *GAPDH*).

For miRNA reactions, the High-Capacity RNA-to-cDNA Kit (Life Technologies) was used for cDNA synthesis from 100 ng of total RNA according to the manufacturer's recommendations. Stem-loop RT primers were synthesized according to Chen et al. (2005) [44]. The cDNA was amplified with universal and forward primers, and the quantifications were normalized using the reference miRNA (U6). All reactions were used using the SYBR Green PCR Master Mix system (Thermo Fisher, USA). The expression level of the selected miRNA and mRNAs was determined using the QuantStudio™ 12K Flex real-time PCR system (Thermo Fisher Scientific) on 96 plate wells. The values were calculated using the expression ratio of the GLLP/CTR groups. The relative quantification of each gene was performed using the $2^{-\Delta\Delta CT}$ method normalized using [45]. For these experiments, the cells that received the lipofectamine vehicle were used as the control group. The sequences of the primers were designed on the Primer Express 3.0 software (Supplementary Table 2).

2.9 In vivo validation: selected miRNA, its predicted target, and hormones receptors in offspring VP

To evaluate the expression profile of these miRNA, the target mRNA and hormones receptors in young (PND21) and older (PND540) offspring rats, the total RNA was extracted from samples (n = 6/group) in all experimental groups and both ages using TRIzol® Reagent (ThermoFisher Scientific) according to the manufacturer's recommendations. The samples of old rats we used were generated in a previous study of our research group [22]. Details of the RT-qPCR reactions were described in item 2.8.3. For the mRNA data, the normalization was conducted using *Gapdh* and *Gusb* as reference genes; for the miRNA data, the normalization was conducted using the reference miRNA (U6). Primer sequences were described in Supplementary Table 2.

2.10 Statistical analysis

Statistical analyses were performed using the GraphPadPrism® software (version 5.00, Graph Pad, Inc., San Diego, CA). The results were submitted to normalization analysis (Shapiro-Wilk test). Parametric data were compared using the Student's t-test. The remaining (dams body weight gain in the lactation, Offspring weight at PND21, DHEA concentration, and *Plg* expression in VP samples) were submitted to Mann-Whitney. Data were expressed as mean ± SD. The differences were considered statistically significant when $p < 0.05$. The statistical tests used are described in the figure legends.

2.11 Data representation and analyses

Bar graphs were generated using the GraphPad Prism tool (GraphPad Software). The heatmap with the results of RT-qPCR was created using the Morpheus web tool (https://software.broadinstitute.org/morpheus) [46]. miRNA-mRNAs networks were demonstrated by circus plot graphics generated in the R environment using the "Circlize" package [47]. The UpSet plot generated to represent deregulated miRNAs in the VP of animals submitted to maternal malnutrition and PCa patients was made on the Intervene platform (https://intervene.shinyapps.io/intervene/) [48]. The

relationships between the molecular pathways and the predicted targets of miRNA, demonstrated in an alluvium diagram, were performed on the Sankeymatic platform (https://sankeymatic.com/).

3. Results

3.1 Maternal malnutrition alters biometrical parameters in dams and offspring

Dams from the GLLP group displayed lower body weight gain during pregnancy and lactation, although the relative food and energy intake did not change compared to the control group (Table 1). The offspring from the GLLP group showed a reduced body weight, reduced anogenital distance at PND 1 and 21, and lower VP absolute and relative weight at PND 21 compared to the CTR group (Table 1).

3.2 Maternal malnutrition affects hormone levels and impairs prostate growth in young male offspring

We observed an increase in total cholesterol and plasma concentrations of testosterone and 17β-estradiol in the GLLP group compared to the CTR group at PND 21. Conversely, plasma concentrations of pregnenolone, progesterone, and DHEA were reduced in the GLLP group (Fig. 1).

The morphological analysis demonstrated an impairment of prostatic growth in the GLLP compared to the CTR group at PND 21 (Figs. 2a and b). We observed a reduction in the lumen of prostatic acini associated with increased collagen deposition in the stromal compartment in the GLLP group compared to the CTR group (Fig. 2c and d). The morphometric data confirmed the impairment of prostatic growth (Fig. 2e). Consistent with the increase in collagen in the stromal compartment, the gelatinolytic activity of the active form of MMP-2 was reduced in the GLLP group compared to the CTR (Fig. 2f).

3.3 Maternal malnutrition alters the miRNA-mRNA networks in the young offspring VP

The integrative analysis identified 49 DE miRNAs (28 up and 21 downregulated) (Supplementary Table 3) and 707 DE mRNA (525 up and 182 downregulated) in the VP from the GLLP group (Supplementary Table 4, Fig. 3a). We evaluated the interaction of 49 DE miRNAs with predicted mRNAs and identified 51,338 potential target mRNAs (Supplementary Table 5). Then, we compared the list of predicted mRNAs with the DE mRNA identified in the VP, resulting in the match of 268 mRNAs potentially regulated by 47 miRNAs (Fig. 3b and Supplementary Table 6), considering miRNAs upregulated and mRNA downregulated and vice versa.

3.4 Similarities between miRNA-mRNA networks in the VP of maternally malnourished offspring and PCa patients

We identified 245 DE miRNAs (118 downregulated and 127 upregulated) in patients diagnosed with PCa using the PRAD-TCGA dataset (Supplementary Table 7). The integrative analysis demonstrated

similarities between eight commonly DE miRNAs in the VP from the GLLP group and patients with PCa (*miR-1-3p, miR-141-3p, miR-184, miR-206-3p, miR-410-3p, miR-452-5p, miR-496-3p, miR-96-5p*) (Fig. 3c). Of these, 5 miRNAs (*miR-141-3p, miR-96-5p, miR-410-3p, miR-184, and miR-206-3p*) shared identical sequences in both human and *Rattus norvegicus* (Supplementary Table 8, Fig. 3d). Based on these results, we selected *rno-miR-206-3p*, which presented a higher fold change among DE miRNAs (1.79) and their predicted target mRNAs (*Zfp366*, *Plg*, *Rimbp2*, *Pbld1*, *Lhfpl2*, *Dtna*, *Rmnd5a*, *Zmat3*, *Mob3b*, *Stxbp6*, *LOC103692716*) for further validations (Supplementary Table 6).

3.5 Molecular pathways enriched by the miR-206/predicted targets

Predicted targets of miR-206 enriched molecular pathways related to the regulation of cell-cell adhesion mediated by cadherin (GO:2000047), regulation of IGF transport and uptake by IGFBPs (R-HSA-381426), activation of matrix metalloproteinases (R-HSA-1592389), regulated exocytosis (GO:0045055), negative regulation of exocytosis (GO:0045920), exocyst localization (GO:0051601) development of primary female sexual characteristics (GO:0046545), negative regulation of intracellular estrogen receptor signaling pathway (GO:0033147), regulation of intracellular estrogen receptor signaling pathway (GO:0033146) estrogen receptor binding (GO:0030331), signal transduction by p53 class mediator (GO:0072331), miRNA regulation of p53 pathway in prostate cancer (WP3982), interleukin 1Î² rat insulinoma cell line (GDS4332 ligand:186). Seven DE mRNAs (*ZNF366*, *PLG*, *ZMAT3*, *RIMBP2*, *PBLD*, *LHFPL2*, and *STXBP6*) were mostly associated with enriched molecular pathways (Fig. 4a).

To further assess the potential role of these seven DE mRNAs in predicting a worse prognosis for PCa (PRAD-TCGA), the SurvExpress tool was used to explore the prognostic index correlating survival analysis and cancer risk assessment. Our set of genes clustered the PCa patients (n = 497) into two distinct groups (at high-risk, n = 128 and low-risk, n = 369), and was strongly associated with shorter survival of patients, as shown in PRAD (hazard ratio (HR) = 9.31; log-rank p-value = 0.001392) (Fig. 4b). Furthermore, data from the HPA database demonstrated the immunolocalization of three targets (*PLG*, *ZNF366*, and *ZMAT3*) in PCa (Fig. 4c).

3.6 Effects of transient transfection of prostatic cells with mimic miR-206

After the identification and *in silico* selection of potential miRNA-mRNA networks altered by maternal malnutrition in the offspring VP, we performed functional assays in benign prostatic PNT2 cells with *miR-206* mimetic molecules attempting to elucidate the impact of increased miR-206 expression in the prostate. Cells transfected with the *miR-206* mimic did not show morphological changes compared to cells treated with lipofectamine (Fig. 5a-b). The *miR-206* expression increased in PNT-2 cells transiently transfected with mimic *miR-206* (Fig. 5c). Interestingly, the expression of *PLG* and ESR1 transcripts decreased in mimic *miR-206*-treated cells (Fig. 5d-e), highlighting the potential *miR-206-PLG-ERS1* interaction. The expression of *ESR2* and *AR* did not change in this condition (Fig. 5f-g). The MTT assays demonstrated a reduction in the viability after 72 h of exposure to mimic *miR-206* compared to the

control cells (Fig. 5h). The wound-healing assay showed that *miR-206* transfected cells delayed wound healing potential after 48 and 72 h of treatment (Fig. 5i-j).

3.7 Validation of miR-206 network in the VP of young and older offspring rats

Consistent with the integrative analysis of RNAseq, *miR-206* was upregulated in the VP of young rats from the GLLP group compared to the CTR group on PND21 (Fig. 6a). In parallel, we observed that *Plg* transcript levels were downregulated in the GLLP group (Fig. 6b). Moreover, we observed an increase in the *Ar* expression (Fig. 6c) and a reduction of *Esr1* and *Esr2* in the VP of young rats from the GLLP group compared to the CTR group (Figs. 6d-e).

To give further insights into the participation of the *miR-206* in the prostate carcinogenesis in the progeny submitted to maternal LPD, RT-qPCR analysis revealed a reduction of *miR-206* expression was observed in the VP of older rats from the GLLP group compared to the CTR group. It was accomplished by an increase of *Plg* expression (Fig. 6f and g). The *Ar* appeared downregulated, while *Esr1* was upregulated, and the *Esr2* did not change in the VP or older rats from the GLLP group compared to the CTR group (Figs. 6h-j).

Figure 7 summarizes the workflow depicting the effects of maternal exposure to a low protein diet on the deregulation of the molecular mechanisms involved in the developmental origins of PCa. We further highlighted the key role of miR206-network and estrogen signaling pathways (through deregulation of ERα) as a potential prostate cancer driver in older offspring submitted to maternal malnutrition.

4. Discussion

Over the past decades, the DOHaD concept has provided causal relationships between early-life exposure to environmental risk factors and the developmental origins of non-communicable chronic diseases, including PCa [7, 21, 22]. Although the molecular mechanisms involved in this process remain elusive, the imbalance of sex hormones in both dams and offspring submitted to maternal malnutrition has been pointed to as a key factor related to prostate carcinogenesis in the progeny [6, 9, 10, 21, 22].

To further elucidate how maternal malnutrition interferes with the balance of sex hormones in male offspring, we evaluated the serum cholesterol profile and their intermediate metabolites involved in the steroidogenesis pathways. An increase in total cholesterol was observed in GLLP animais at PND 21. Sohi et al. (2011) have demonstrated an increase in cholesterol levels in male rat offspring submitted to MPR (8% protein) at the same age and associated this result with permanent epigenetic silencing of the hepatic *Cyp7a1* promoter, which metabolizes cholesterol to bile acids [49]. The offspring from the GLLP group also showed an imbalaced in plasma concentrations of steroid hormones; while testosterone and estradial were elevated, pregnenolone, progesterone, and DHEA were reduced, suggesting that these intermediate metabolites could be consumed to sustain the higher levels of testosterone and estradiol.

Although largely driven by androgens, the developing prostate is sensitive to estrogens. Epidemiological and experimental data have demonstrated that abnormal exposure to an excessive estrogenization early in life may disrupt molecular mechanisms governing prostate developmental biology, with long-lasting consequences for prostate diseases with aging [9, 21, 22, 50]. As such, African-American men are at higher risk of prostatic carcinoma than their Caucasian counterparts, and it has been postulated that this higher risk is related, in part, to the higher estrogens levels observed during pregnancy in the former population [9, 10]. These conditions, termed "developmental estrogenization" or "estrogen imprinting", states that inappropriate exposure to estrogen (due to ethnicity, exposure to the endocrine disruptor, environmental chemicals, maternal malnutrition, among other individual and environmental factors) is memorized ("imprinted") by cells and tissues [12, 13, 51–56]. Understanding the relationship between exposure to an estrogenic environment with long-lasting consequences for prostate diseases is essential for the DOHaD concept. It has been demonstrated in rodent models that exposure to high levels of estrogens early in life blocks epithelial cell differentiation and increases the number of basal epithelial cells [15, 57]. Using proteomic approaches, Santos et al., 2020 identified estrogenic signaling pathways, endoplasmic reticulum functions, oxidative stress, and deregulation of insulin/IGF signaling pathways as the main deregulated mechanisms involved in the VP response to maternal malnutrition in both young and older male offspring [23]. We further demonstrated that the impairment of the glandular compartment in young rats was associated with an increase in collagen fiber deposition in the stroma. The increase in collagen content can be explained, at least in part, by the reduction of the gelatinolytic activity of the active form of the MMP-2, a class of enzyme responsible for extracellular matrix remodeling in the prostate gland [27, 58, 59].

To give further translational insights into the relationship between deregulated miRNAs networks early in life and the developmental origins of PCa, we identified 5 miRNAs with similar nucleotide sequences commonly deregulated in the VP of maternally malnourished offspring and patients with PCa. Of these, miR-206 was selected for further functional validation. RT-qPCR confirmed the upregulation of this miRNA in the VP of young offspring. Accordingly, experimental upregulation of *miR-206* led to retardation of mammary gland development through modulation of *Wnt* and transcription factors *Tbx3* and *Lef1* [60]. The upregulation of *miR-206* in the GLLP group can be associated with stromal collagen accumulation in the impaired VP of young rats since the *miR-206/Plg* network, which modulates the extracellular matrix remodeling and angiogenesis processes [61, 62], was downregulated in these animals.

It is noteworthy that the prostate is particularly more sensitive to estrogens during critical windows of development [12]. Estrogen actions on the prostate are mainly mediated through major canonical estrogen receptors (ER), including ERα and ERβ. Studies involving knockout mice and developmental exposure to estrogenic compounds indicate that paracrine signaling involving stromal ERα is the dominant form of estrogen-mediated imprinting in the developing uterus [63], ovary [63], mammary gland [64], lung [65], and prostate [51, 66, 67]. Consistently, the deletion of the ERα gene in the stromal fibroblast leads to a reduction in prostate branching morphogenesis [66]. Additionally, Lee et al., (2013) demonstrated that *miR-206* epigenetically regulates downregulated *ESR1* expression during normal

mammary gland development [60]. Although there is no data regarding the *Esr1* modulation by miR-206 in the developing prostate, our data demonstrated the potential relationship of *miR-206* in modulating ER signaling since *miR-206*-ERs networks have opposite expression profiles in the VP of young offspring in the GLLP group.

In addition to the miR-206 potential role as an important modulator of gene expression during the developmental process, a body of evidence highlighted its key role as a tumor suppressor miRNA in PCa [35, 36, 64]. However, there is no data regarding the epigenetic modulation of ERs by miR-206 in PCa. Studies with knockout mice for estrogen receptors indicate that *Esr1* and *Esr2* can have opposite actions on prostate carcinogenesis since *Esr1* is recognized to promote cell proliferation, while *Esr2* has been described as anti-proliferative and proapoptotic. Altogether, these results suggest that the overall proliferative response to estrogen results from a balance between ERα and ERβ signaling [68–70]. Our functional validation experiments demonstrated downregulation of *ESR1* expression in PNT2 cells transfected with *miR-206*. These results are consistent with deregulation of the *miR-206-ESR1* network observed in the VP of young and older offspring rats from the GLLP group. Moreover, it has been demonstrated that *in vitro* inhibition of *miR-206* in PC-3 cells increases cell invasion through upregulated ANXA2 and E-cadherin, and downregulation of N-cadherin and vimentin [35]. Wang et al., (2018) also described the tumor suppressor effect of miR-206 in PCa by negatively regulating cell proliferation and migration by targeting *CXCL11* [64]. These authors also demonstrated experimentally that up-regulation of *miR-206* inhibits proliferation, migration, invasion, and induced G1/G0 arrest of PCa cells. The expression profile of miRNA extracted from PRAD-TCGA demonstrated the downregulation of *miR*-206 in patients with PCa. Interestingly, we observed a reduction in the expression profile of *miR-206* and an increase in *Plg* gene expression in the VP of older offspring rats from the GLLP groups, which developed prostate carcinoma *in situ* [22–24]. Functional validation confirmed the modulation negative correlation of the miR-206/PLG expression, as well as their participation in modulating cell migration and invasion in PNT2 cells. Furthermore, we provide new evidence on the participation of *miR*206-ESR1 network mediating prostate carcinogenesis in maternally malnourished offspring rats. Overall, our data provide new insights into the participation of an estrogenized environment associated with deregulation of miR-206-PLG-ESR1 in the developmental origin of prostate diseases in maternally malnourished offspring rats. Understanding these mechanisms can encourage the adoption of a governmental policy for the early life prevention of non-communicable chronic diseases, as proposed by the DOHaD concept.

Declarations

Funding: Sao Paulo State Research Foundation FAPESP (2018/26120-6; 2017/01063-7; 2021/03405-8) and National Council for Scientific and Technological Development (CNPq grant # 310,663/2018–0).

Author contributions: All authors contributed to the study conception and design. LMFP and LAJ designed the project, performed the conceptualization, animal experimentation, methodology, analyses, interpretation of data, and wrote the manuscript. Material preparation, data collection, and analyses were performed by LMFP, FBC, ACLC, SAAS, LAB, MNF, WRS, and KTC. The first draft of the manuscript was

written by LMFP, LAJ, EJRS, and CSM. All authors commented on previous versions of the manuscript. All authors read and approved the final manuscript.

Conflict of interest: The authors declare no competing financial interests.

Availability of data and material: The datasets presented in this study can be found in online repositories on The Cancer Genome Atlas (TCGA) projects; The Gene Expression Omnibus (GEO) on accession number(s) GSE180673 and GSE180674.

Ethics approval: This study was performed in line with the principles ethics. Approval was granted by the Biosciences Institute/UNESP Ethics Committee for Animal Experimentation (Protocol #1178).

Code availability: Not applicable.

References

1. WHO WHO (2021) World Health Organization, Health Topics: Nutrition. https://www.who.int/health-topics/nutrition. Accessed 31 Aug 2021
2. Gluckman PD, Hanson MA, Pinal C (2005) The developmental origins of adult disease. Matern Child Nutr 1:130. https://doi.org/10.1111/J.1740-8709.2005.00020.X
3. Gluckman PD, Hanson MA, Mitchell MD (2010) Developmental origins of health and disease: reducing the burden of chronic disease in the next generation. Genome Med 2:14. https://doi.org/10.1186/GM135
4. Barker DJP, Osmond C (1986) Infant mortality, childhood nutrition, and ischaemic heart disease in England and Wales. Lancet (London England) 1:1077–1081. https://doi.org/10.1016/S0140-6736(86)91340-1
5. Barker DJP, Osmond C, Thornburg KL et al (2012) A possible link between the pubertal growth of girls and prostate cancer in their sons. Am J Hum Biol 24:406–410. https://doi.org/10.1002/AJHB.22222
6. Gardner WA (1995) Hypothesis: the prenatal origins of prostate cancer. Hum Pathol 26:1291–1292. https://doi.org/10.1016/0046-8177(95)90291-0
7. Keinan-Boker L, Vin-Raviv N, Liphshitz I et al (2009) Cancer incidence in Israeli Jewish survivors of World War II. J Natl Cancer Inst 101:1489–1500. https://doi.org/10.1093/JNCI/DJP327
8. Trichopoulos D (1990) Hypothesis: does breast cancer originate in utero? Lancet. (London England) 335:939–940. https://doi.org/10.1016/0140-6736(90)91000-Z
9. Powell IJ, Meyskens FL (2001) African American men and hereditary/familial prostate cancer: Intermediate-risk populations for chemoprevention trials. Urology 57:178–181. https://doi.org/10.1016/S0090-4295(00)00968-7
10. Henderson BE, Bernstein L, Ross RK et al (1988) The early in utero oestrogen and testosterone environment of blacks and whites: potential effects on male offspring. Br J Cancer 57:216. https://doi.org/10.1038/BJC.1988.46

11. Nelles JL, Hu WY, Prins GS (2011) Estrogen action and prostate cancer. Expert Rev Endocrinol Metab 6:437–451. https://doi.org/10.1586/EEM.11.20
12. Prins GS, Birch L, Tang WY, Ho SM (2007) Developmental estrogen exposures predispose to prostate carcinogenesis with aging. Reprod Toxicol 23:374–382. https://doi.org/10.1016/J.REPROTOX.2006.10.001
13. Cheong A, Zhang X, Cheung YY et al (2016) DNA methylome changes by estradiol benzoate and bisphenol A links early-life environmental exposures to prostate cancer risk. Epigenetics 11:674–689. https://doi.org/10.1080/15592294.2016.1208891
14. Scarano WR, Bedrat A, Alonso-Costa LG et al (2019) Exposure to an environmentally relevant phthalate mixture during prostate development induces microRNA upregulation and transcriptome modulation in rats. Toxicol Sci 171:84–97. https://doi.org/10.1093/TOXSCI/KFZ141
15. Colombelli KT, Santos SAA, Camargo ACL et al (2017) Impairment of microvascular angiogenesis is associated with delay in prostatic development in rat offspring of maternal protein malnutrition. Gen Comp Endocrinol 246:258–269. https://doi.org/10.1016/J.YGCEN.2016.12.016
16. Rinaldi JC, Justulin LA, Lacorte LM et al (2013) Implications of intrauterine protein malnutrition on prostate growth, maturation and aging. Life Sci 92:763–774. https://doi.org/10.1016/J.LFS.2013.02.007
17. Pinho CF, Ribeiro MA, Rinaldi JC et al (2014) Gestational protein restriction delays prostate morphogenesis in male rats. Reprod Fertil Dev 26:967–973. https://doi.org/10.1071/RD13132
18. Harrath AH, Alrezaki A, Alwasel SH, Semlali A (2019) Intergenerational response of steroidogenesis-related genes to maternal malnutrition. J Dev Orig Health Dis 10:587–594. https://doi.org/10.1017/S2040174419000060
19. Lea RG, Andrade LP, Rae MT et al (2006) Effects of maternal undernutrition during early pregnancy on apoptosis regulators in the ovine fetal ovary. Reproduction 131:113–124. https://doi.org/10.1530/REP.1.00844
20. Edwards LJ, Bryce AE, Coulter CL, McMillen IC (2002) Maternal undernutrition throughout pregnancy increases adrenocorticotrophin receptor and steroidogenic acute regulatory protein gene expression in the adrenal gland of twin fetal sheep during late gestation. Mol Cell Endocrinol 196:1–10. https://doi.org/10.1016/S0303-7207(02)00256-3
21. Portela LM, Santos SA, Constantino FB et al (2021) Increased oxidative stress and cancer biomarkers in the ventral prostate of older rats submitted to maternal malnutrition. Mol Cell Endocrinol 523. https://doi.org/10.1016/J.MCE.2020.111148
22. Santos SAA, Camargo AC, Constantino FB et al (2019) Maternal Low-Protein Diet Impairs Prostate Growth in Young Rat Offspring and Induces Prostate Carcinogenesis With Aging. J Gerontol A Biol Sci Med Sci 74:751–759. https://doi.org/10.1093/GERONA/GLY118
23. Santos SAA, Lima Camargo AC, Constantino FB et al (2020) Identification of potential molecular pathways involved in prostate carcinogenesis in offspring exposed to maternal malnutrition. Aging 12:19954–19978. https://doi.org/10.18632/AGING.104093

24. Bianco-Miotto T, Craig JM, Gasser YP et al (2017) Epigenetics and DOHaD: from basics to birth and beyond. J Dev Orig Health Dis 8:513–519. https://doi.org/10.1017/S2040174417000733
25. Reeves PG, Nielsen FH, Fahey GC (1993) AIN-93 purified diets for laboratory rodents: final report of the American Institute of Nutrition ad hoc writing committee on the reformulation of the AIN-76A rodent diet. J Nutr 123:1939–1951. https://doi.org/10.1093/JN/123.11.1939
26. Fischbeck KL, Rasmussen KM (1987) Effect of repeated reproductive cycles on maternal nutritional status, lactational performance and litter growth in ad libitum-fed and chronically food-restricted rats. J Nutr 117:1967–1975. https://doi.org/10.1093/JN/117.11.1967
27. Justulin LA, Della-Coleta HHM, Taboga SR, Felisbino SL (2010) Matrix metalloproteinase (MMP)-2 and MMP-9 activity and localization during ventral prostate atrophy and regrowth. Int J Androl 33:696–708. https://doi.org/10.1111/J.1365-2605.2009.01016.X
28. Bradford M (1976) A rapid and sensitive method for the quantitation of microgram quantities of protein utilizing the principle of protein-dye binding. Anal Biochem 72:248–254. https://doi.org/10.1006/ABIO.1976.9999
29. Love MI, Huber W, Anders S (2014) Moderated estimation of fold change and dispersion for RNA-seq data with DESeq2. Genome Biol 15:1–21. https://doi.org/10.1186/S13059-014-0550-8/FIGURES/9
30. Sticht C, De La Torre C, Parveen A, Gretz N (2018) miRWalk: An online resource for prediction of microRNA binding sites. PLoS ONE 13. https://doi.org/10.1371/JOURNAL.PONE.0206239
31. Kozomara A, Birgaoanu M, Griffiths-Jones S (2019) miRBase: from microRNA sequences to function. Nucleic Acids Res 47:D155–D162. https://doi.org/10.1093/NAR/GKY1141
32. Griffiths-Jones S, Grocock RJ, van Dongen S et al (2006) miRBase: microRNA sequences, targets and gene nomenclature. Nucleic Acids Res 34. https://doi.org/10.1093/NAR/GKJ112
33. Yang N, Wang L, Liu J et al (2018) MicroRNA-206 regulates the epithelial-mesenchymal transition and inhibits the invasion and metastasis of prostate cancer cells by targeting Annexin A2. Oncol Lett 15:8295. https://doi.org/10.3892/OL.2018.8395
34. Chua FY, Adams BD (2017) Androgen receptor and miR-206 regulation in prostate cancer. Transcription 8:313. https://doi.org/10.1080/21541264.2017.1322668
35. Kuleshov MV, Jones MR, Rouillard AD et al (2016) Enrichr: a comprehensive gene set enrichment analysis web server 2016 update. Nucleic Acids Res 44:W90–W97. https://doi.org/10.1093/NAR/GKW377
36. Chen EY, Tan CM, Kou Y et al (2013) Enrichr: Interactive and collaborative HTML5 gene list enrichment analysis tool. BMC Bioinformatics 14:1–14. https://doi.org/10.1186/1471-2105-14-128/FIGURES/3
37. Aguirre-Gamboa R, Gomez-Rueda H, Martínez-Ledesma E et al (2013) SurvExpress: An Online Biomarker Validation Tool and Database for Cancer Gene Expression Data Using Survival Analysis. PLoS ONE 8:74250. https://doi.org/10.1371/JOURNAL.PONE.0074250
38. Pontén F, Jirström K, Uhlen M (2008) The Human Protein Atlas–a tool for pathology. J Pathol 216:387–393. https://doi.org/10.1002/PATH.2440

39. Berglund L, Björling E, Oksvold P et al (2008) A genecentric Human Protein Atlas for expression profiles based on antibodies. Mol Cell Proteomics 7:2019–2027. https://doi.org/10.1074/MCP.R800013-MCP200
40. Uhlen M, Zhang C, Lee S et al (2017) A pathology atlas of the human cancer transcriptome. Science 357. https://doi.org/10.1126/SCIENCE.AAN2507
41. Berridge MV, Tan AS (1993) Characterization of the cellular reduction of 3-(4,5-dimethylthiazol-2-yl)-2,5-diphenyltetrazolium bromide (MTT): subcellular localization, substrate dependence, and involvement of mitochondrial electron transport in MTT reduction. Arch Biochem Biophys 303:474–482. https://doi.org/10.1006/ABBI.1993.1311
42. Mosmann T (1983) Rapid colorimetric assay for cellular growth and survival: application to proliferation and cytotoxicity assays. J Immunol Methods 65:55–63. https://doi.org/10.1016/0022-1759(83)90303-4
43. Freire PP, Cury SS, De Oliveira G et al (2017) Osteoglycin inhibition by microRNA miR-155 impairs myogenesis. PLoS ONE 12. https://doi.org/10.1371/JOURNAL.PONE.0188464
44. Chen C, Ridzon DA, Broomer AJ et al (2005) Real-time quantification of microRNAs by stem–loop RT–PCR. Nucleic Acids Res 33:e179–e179. https://doi.org/10.1093/NAR/GNI178
45. Livak KJ, Schmittgen TD (2001) Analysis of relative gene expression data using real-time quantitative PCR and the 2(-Delta Delta C(T)) Method. Methods 25:402–408. https://doi.org/10.1006/METH.2001.1262
46. Starruß J, De Back W, Brusch L, Deutsch A (2014) Morpheus: a user-friendly modeling environment for multiscale and multicellular systems biology. Bioinformatics 30:1331–1332. https://doi.org/10.1093/BIOINFORMATICS/BTT772
47. Gu Z, Gu L, Eils R et al (2014) circlize Implements and enhances circular visualization in R. Bioinformatics 30:2811–2812. https://doi.org/10.1093/BIOINFORMATICS/BTU393
48. Khan A, Mathelier A (2017) Intervene: A tool for intersection and visualization of multiple gene or genomic region sets. BMC Bioinformatics 18:1–8. https://doi.org/10.1186/S12859-017-1708-7/TABLES/1
49. Sohi G, Marchand K, Revesz A et al (2011) Maternal Protein Restriction Elevates Cholesterol in Adult Rat Offspring Due to Repressive Changes in Histone Modifications at the Cholesterol 7α-Hydroxylase Promoter. Mol Endocrinol 25:785. https://doi.org/10.1210/ME.2010-0395
50. Prins GS, Tang WY, Belmonte J, Ho SM (2008) Developmental exposure to bisphenol A increases prostate cancer susceptibility in adult rats: epigenetic mode of action is implicated. Fertil Steril 89. https://doi.org/10.1016/J.FERTNSTERT.2007.12.023
51. Prins GS, Birch L, Couse JF et al (2001) Estrogen Imprinting of the Developing Prostate Gland Is Mediated through Stromal Estrogen Receptor α. Cancer Res 61:6089 LP – 6097
52. Prins GS, Huang L, Birch L, Pu Y (2006) The role of estrogens in normal and abnormal development of the prostate gland. Ann N Y Acad Sci 1089:1–13. https://doi.org/10.1196/ANNALS.1386.009

53. Prins GS (2008) Estrogen imprinting: when your epigenetic memories come back to haunt you. Endocrinology 149:5919–5921. https://doi.org/10.1210/EN.2008-1266
54. Söder O (2005) Perinatal imprinting by estrogen and adult prostate disease. Proc Natl Acad Sci U S A 102:1269–1270. https://doi.org/10.1073/PNAS.0409703102
55. Singh J, Handelsman DJ (1999) Imprinting by Neonatal Sex Steroids on the Structure and Function of the Mature Mouse Prostate. Biol Reprod 61:200–208. https://doi.org/10.1095/BIOLREPROD61.1.200
56. Ho SM, Tang WY, De Belmonte J, Prins GS (2006) Developmental exposure to estradiol and bisphenol A increases susceptibility to prostate carcinogenesis and epigenetically regulates phosphodiesterase type 4 variant 4. Cancer Res 66:5624–5632. https://doi.org/10.1158/0008-5472.CAN-06-0516
57. Chang WY, Wilson MJ, Birch L, Prins GS (1999) Neonatal estrogen stimulates proliferation of periductal fibroblasts and alters the extracellular matrix composition in the rat prostate. Endocrinology 140:405–415. https://doi.org/10.1210/ENDO.140.1.6401
58. Wilson MJ, Garcia B, Woodson M, Sinha AA (1993) Gelatinolytic and caseinolytic proteinase activities in the secretions of the ventral, lateral, and dorsal lobes of the rat prostate. Biol Reprod 48:1174–1184. https://doi.org/10.1095/BIOLREPROD48.5.1174
59. Wilson MJ (1995) Proteases in prostate development, function, and pathology. Microsc Res Tech 30:305–318. https://doi.org/10.1002/JEMT.1070300406
60. Lee MJ, Yoon KS, Cho KW et al (2013) Expression of miR-206 during the initiation of mammary gland development. Cell Tissue Res 353:425–433. https://doi.org/10.1007/S00441-013-1653-3
61. Pepper MS (2001) Role of the Matrix Metalloproteinase and Plasminogen Activator–Plasmin Systems in Angiogenesis. Arterioscler Thromb Vasc Biol 21:1104–1117. https://doi.org/10.1161/HQ0701.093685
62. Lin CY, Lee HC, Fu CY et al (2013) miR-1 and miR-206 target different genes to have opposing roles during angiogenesis in zebrafish embryos. Nat Commun 2013 41 4:1–11. https://doi.org/10.1038/ncomms3829
63. Couse JF, Korach KS (1999) Estrogen receptor null mice: what have we learned and where will they lead us? Endocr Rev 20:358–417. https://doi.org/10.1210/EDRV.20.3.0370
64. Förster C, Mäkela S, Wärri A et al (2002) Involvement of estrogen receptor beta in terminal differentiation of mammary gland epithelium. Proc Natl Acad Sci U S A 99:15578–15583. https://doi.org/10.1073/PNAS.192561299
65. Morani A, Barros RPA, Imamov O et al (2006) Lung dysfunction causes systemic hypoxia in estrogen receptor beta knockout (ERbeta-/-) mice. Proc Natl Acad Sci U S A 103:7165–7169. https://doi.org/10.1073/PNAS.0602194103
66. Chen M, Yeh CR, Shyr CR et al (2012) Reduced prostate branching morphogenesis in stromal fibroblast, but not in epithelial, estrogen receptor α knockout mice. Asian J Androl 14:546. https://doi.org/10.1038/AJA.2011.181

67. Weihua Z, Mäkelä S, Andersson LC et al (2001) A role for estrogen receptor beta in the regulation of growth of the ventral prostate. Proc Natl Acad Sci U S A 98:6330–6335. https://doi.org/10.1073/PNAS.111150898
68. SÍusarz A, Jackson GA, Day JK et al (2012) Aggressive prostate cancer is prevented in ERαKO mice and stimulated in ERβKO TRAMP mice. Endocrinology 153:4160–4170. https://doi.org/10.1210/EN.2012-1030
69. Giroux V, Bernatchez G, Carrier JC (2011) Chemopreventive effect of ERβ-Selective agonist on intestinal tumorigenesis in Apc(Min/+) mice. Mol Carcinog 50:359–369. https://doi.org/10.1002/MC.20719
70. Heldring N, Pike A, Andersson S et al (2007) Estrogen receptors: how do they signal and what are their targets. Physiol Rev 87:905–931. https://doi.org/10.1152/PHYSREV.00026.2006

Table

Table 1. Biometric parameters of dams and offspring submitted to low protein diet during gestation and lactation.

Parameters	CTR group	GLLP group
Dams body weight gain during pregnancy (g)	47.25 ± 5.99 [a]	37.38 ± 5.02 [b]
Dams body weight gain in the lactation (g)	-0.28 ± 6.70 [a]	-30.44 ± 7.74 [b]
Dams energy intake during pregnancy and lactation (KJ/day)	310.30 ± 22.01	326.20 ± 61.38
Offspring weight at PND1 (g)	7.12 ± 0.55 [a]	5.91 ± 0.57 [b]
AGD at PND1 (mm)	3.30 ± 0.40 [a]	2.89 ± 0.48 [b]
Offspring weight at PND21 (g)	37.23 ± 6.57 [a]	20.03 ± 3.88 [b]
Absolute VP weight at PND21 (mg)	3.24 ± 0.83 [a]	1.440 ± 0.39 [b]
Relative VP weight at PV 21	0.92 ± 0.19 [a]	0.7893 ± 0.16 [b]
AGD at PND21 (mm)	10.69 ± 2.55 [a]	7.64 ± 1.62 [b]

The different letters mean statistical difference between experimental groups with $p < 0.05$. AGD: anogenital distance; VP: ventral prostate; PND: postnatal day; g: grams; KJ: kilojoule; mm: millimeters; mg: milligram; pg: picogram; ng: nanogram.

Figures

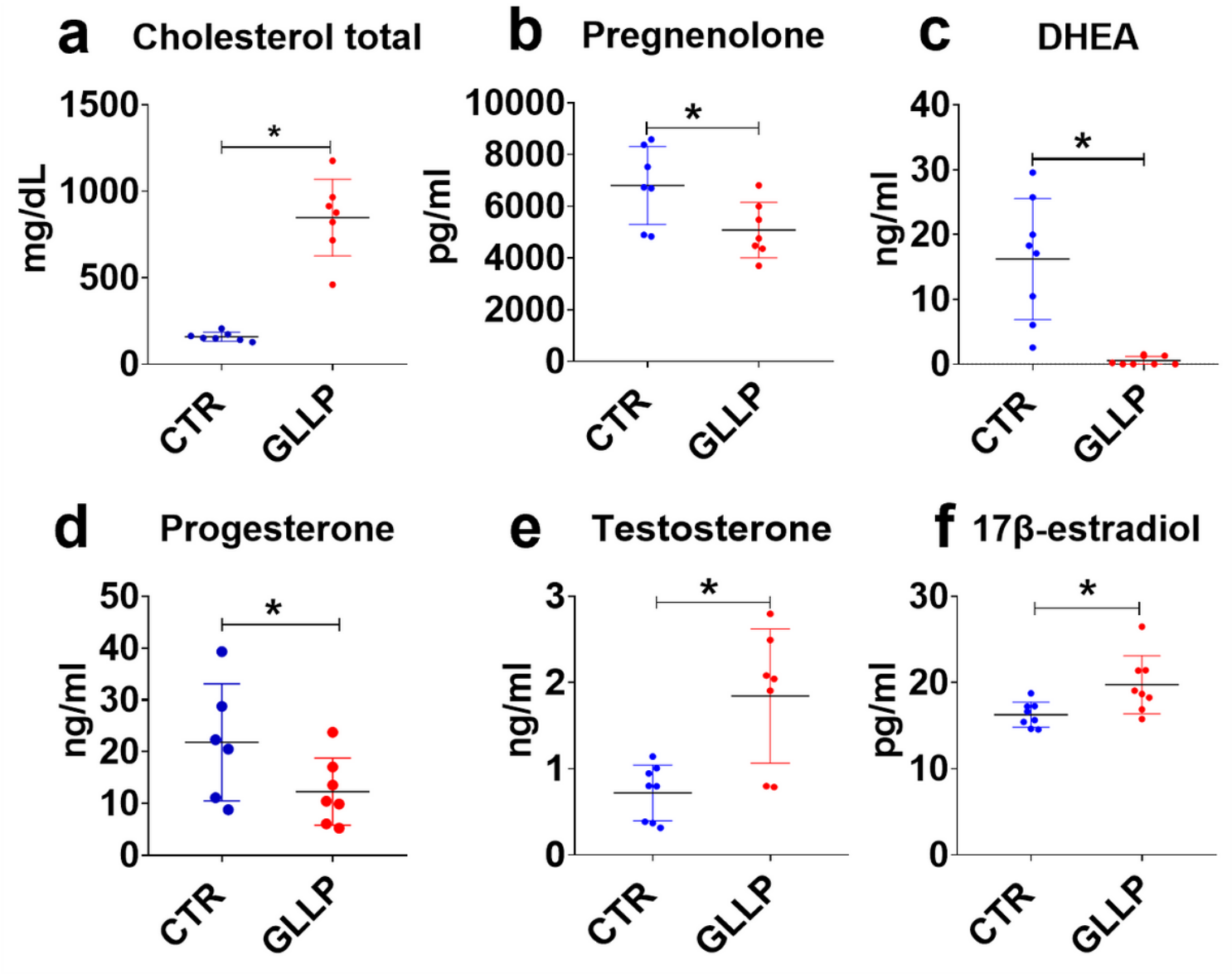

Figure 1

Quantification of serum levels of steroid hormones in animals on a postnatal day (PND) 21 (n=8/per group). Total Cholesterol (a), Pregnenolone (b), Dehydroepiandrosterone (DHEA) (c), Progesterone (d), 17β-hydroxy-4-androstene-3-one (testosterone) (e), 17β-estradiol (f). Data are expressed as mean ± SD. *Signifies a statistical difference between experimental groups with $p < 0.05$.

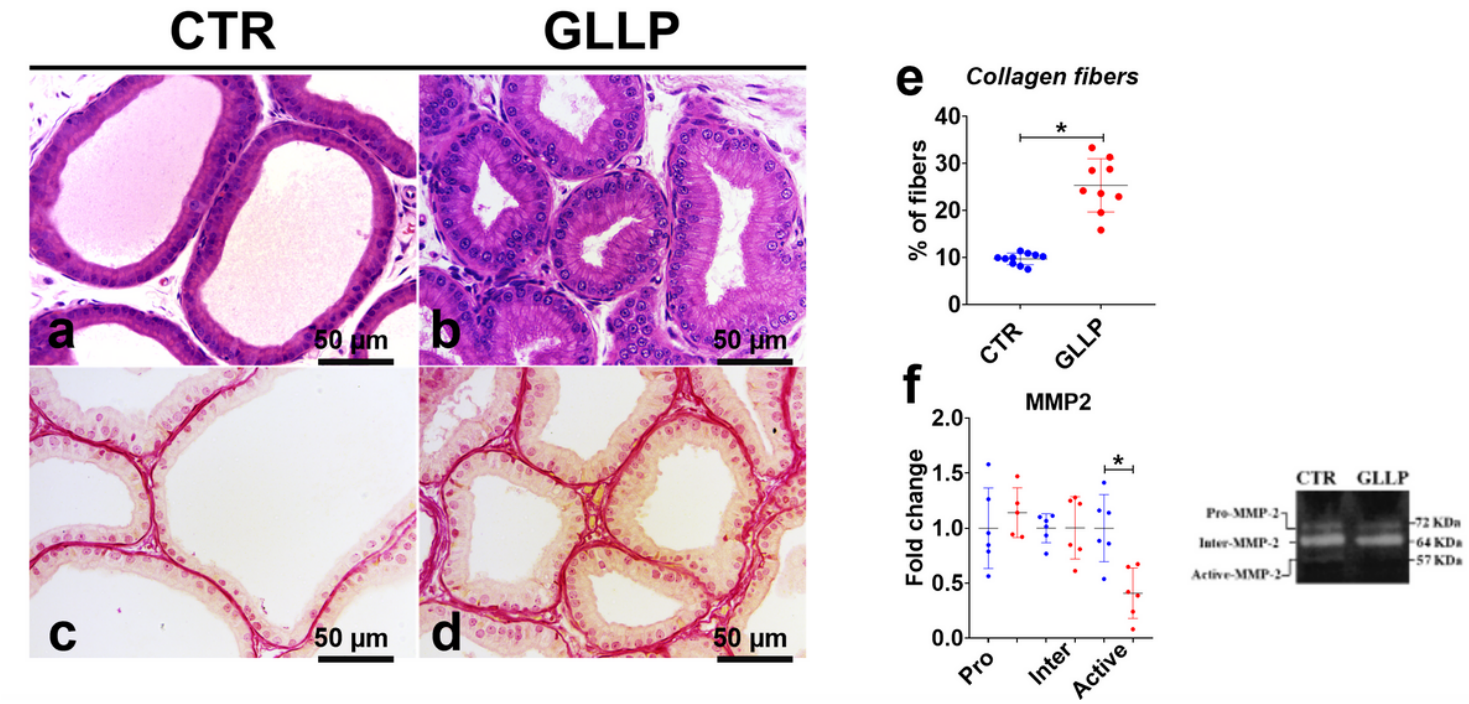

Figure 2

Maternal low protein diet negatively regulated prostate growth in offspring at postnatal day 21 (a-d). Histological sections of the ventral prostate (VP) lobes from the CTR (c, and c) and the GLLP group (b, and d) stained with hematoxylin-eosin (HE) (a-b) or picro sirius red (c-d). Collagen quantification was represented in the bar graph (e). Representative gelatin zymography of the VP demonstrating the gelatinolytic activity of pro, intermediate and active forms of MMP-2 (f). Data are expressed as mean ± SD. *means the statistical difference between experimental groups with $p < 0.05$. Scale bar 50 µm.

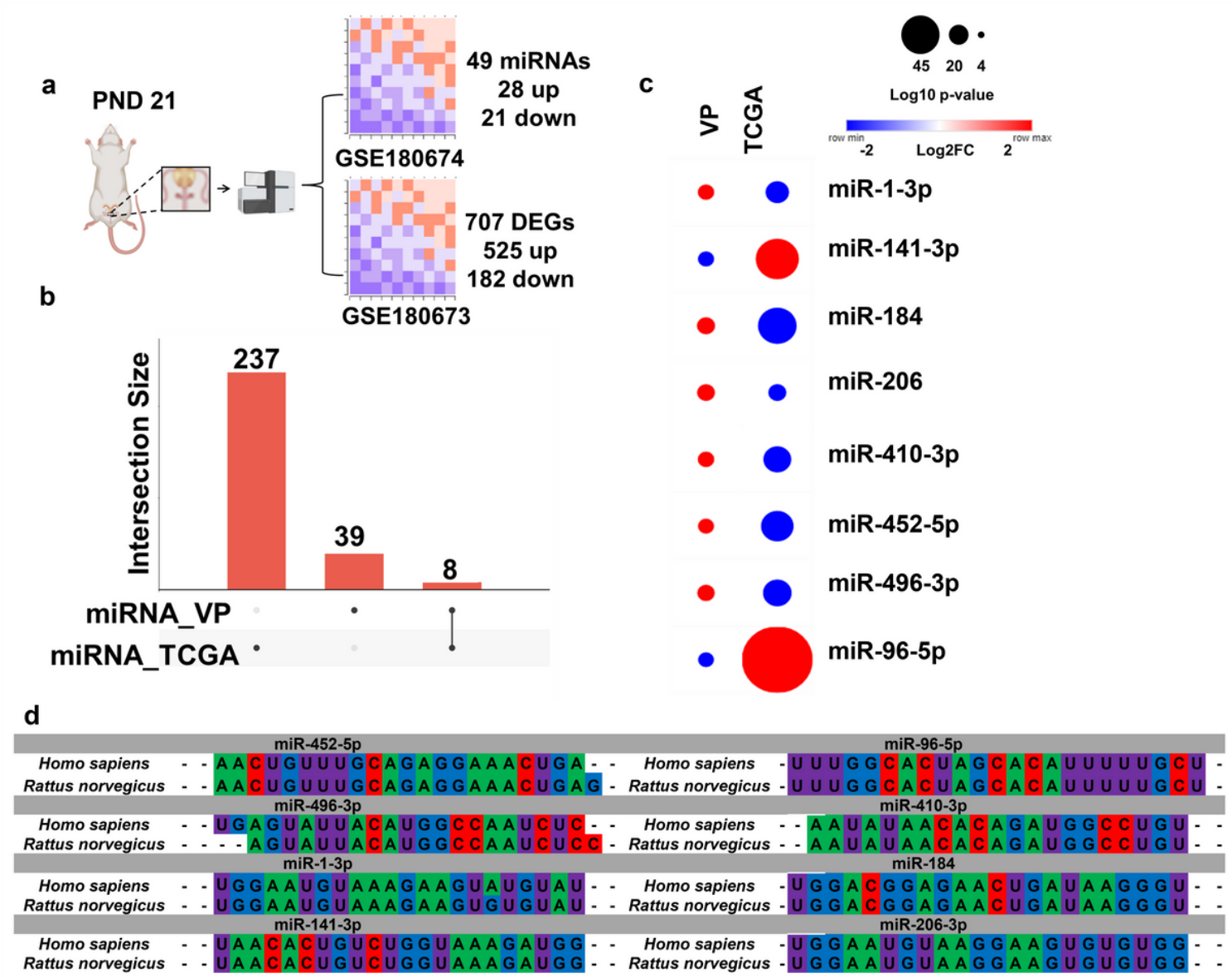

Figure 3

Representative image of bioinformatics analyses. MicroRNome (GSE180674) and transcriptome (GSE180673) datasets from young rat VP were reanalyzed using the DESEq2 package. Differentially expressed targets were considered when p-value < 0.05 and Log2 Fold Change ≥ |+0.66≤|-0.66| (a). Up-set plot showing commonly deregulated miRNAs in the VP from the GLLP group and in patients with PCa (b). Heatmap showing the expression of deregulated miRNAs shared in the VP from the GLLP group with those from PCa patients (c). Sequence alignment of commonly deregulated miRNAs in the PV from the GLLP and in PCa samples. The sequences were obtained through the miRBase database (https://www.mirbase.org/) (d).

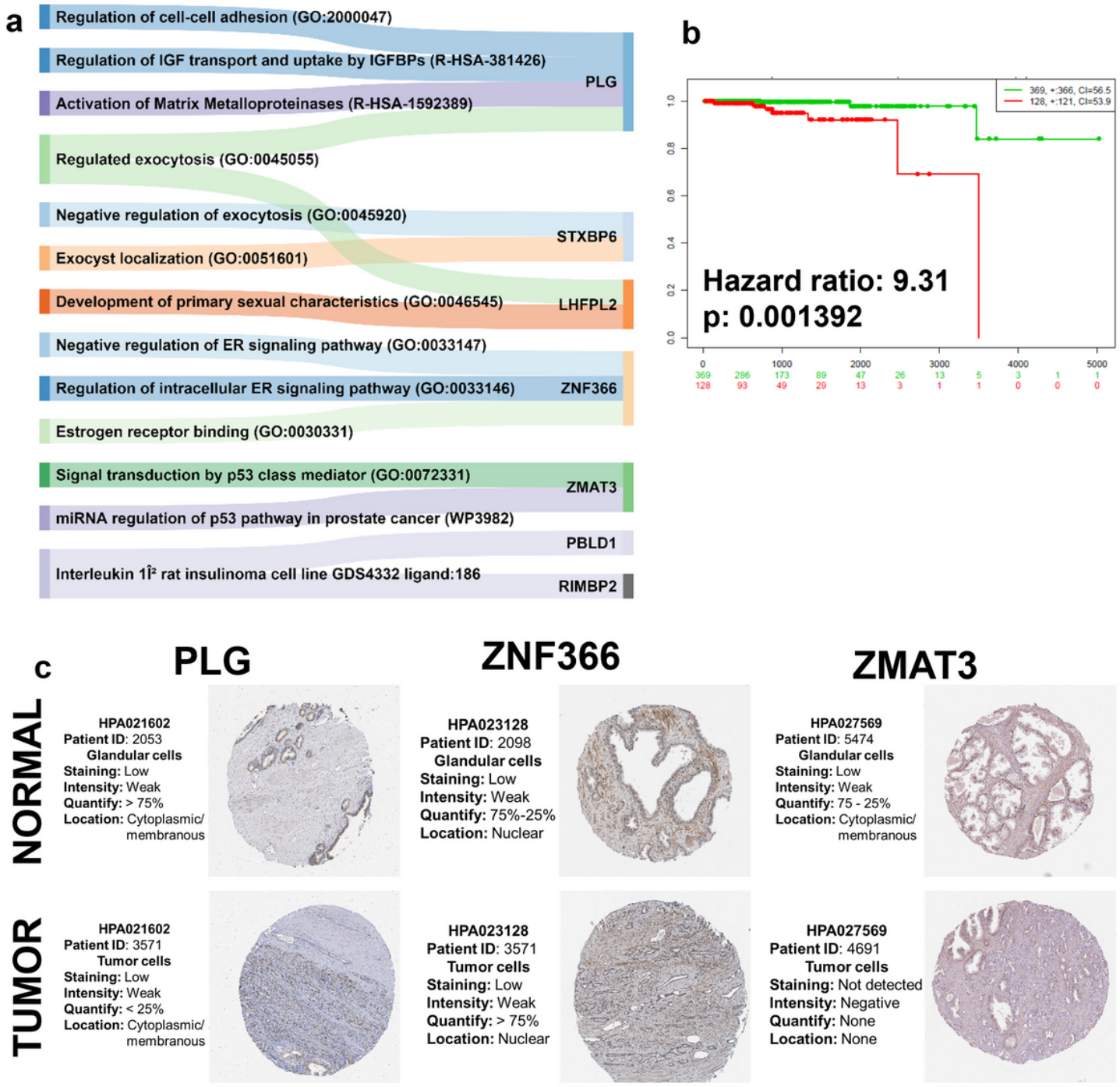

Figure 4

Exploratory analyses of molecular pathways related to the *miR-206* predicted targets. Alluvial diagram showing the relationship between the main molecular pathways and enriched ontological terms for the predicted targets of *miR-206*, these analyzes were performed on the Enrichr platform (https://maayanlab.cloud/Enrichr/), considering p-value < 0.05 (a). Survival curves of PRAD patients (using the TCGA dataset) showing the impact of *miR-206* predicted targets on the stratification of cancer patients in high (red) and low (green) risk (b). Immunohistochemical localization of *PLG*, *ZNF366*, and

ZMAT3 in normal and PRAD tissues obtained from The Human Protein Atlas database (https://proteinatlas.org/) (c).

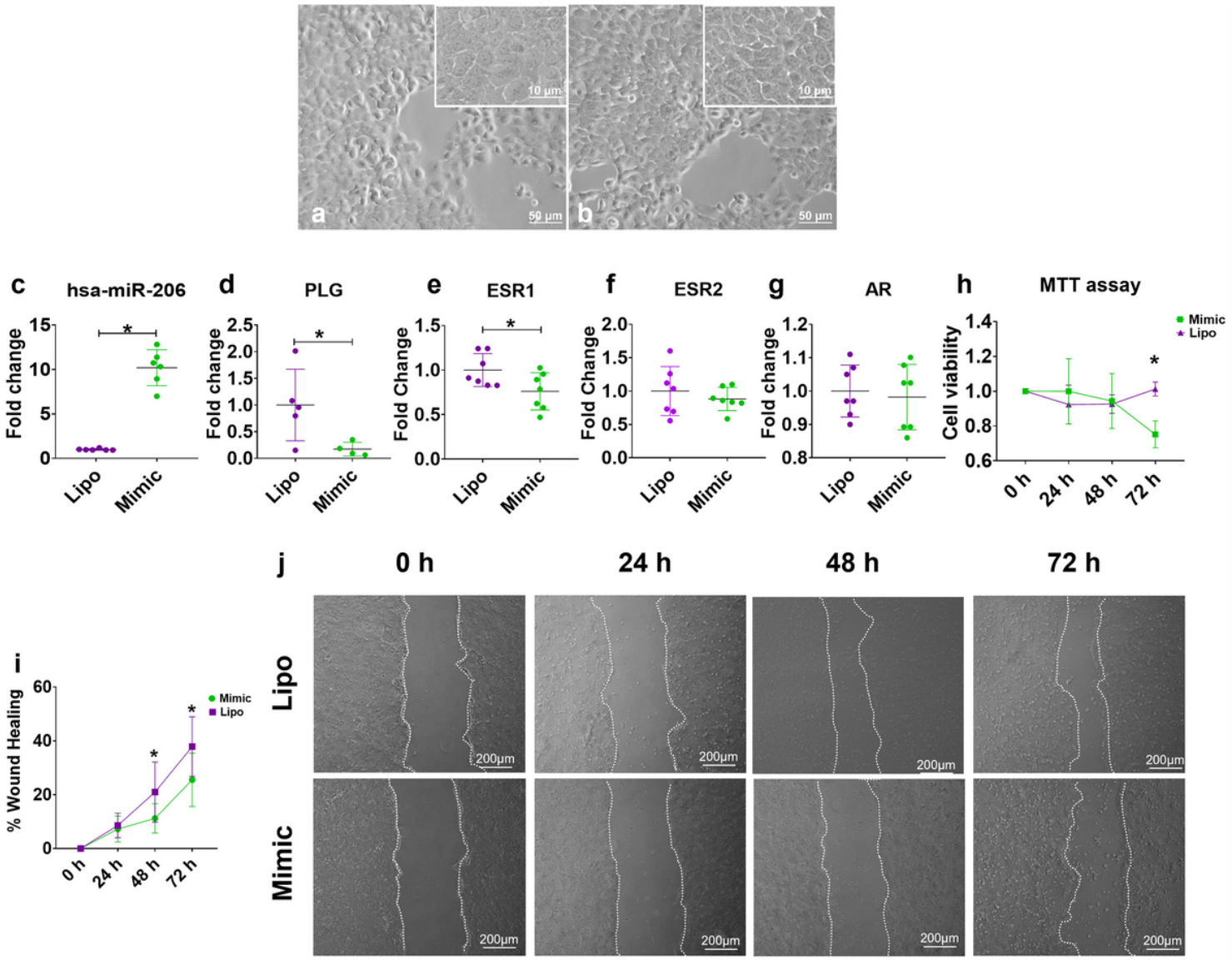

Figure 5

Functional validation of *miR-206* in PNT2 benign prostatic cells. Morphologic aspects of the PNT2 cells in Lipo (a) and Mimic (c) groups after 24 hours of treatment. Expression profile of *miR-206* in PNT2 cells in both experimental groups after 24 hours of treatment (c). *PLG* (d), *ESR1* (e), *ESR2* (f), and *AR* (g) expression levels in PNT2 cells after 24 hours of treatment in both experimental groups. Cell viability assay (MTT) after 24, 48, and 72 hours (h). Representative images of wound healing assay after 24, 48, and 72 hours (i). Cellular wound closure after the transfection of PNT2 cells with Lipo and Mimic groups after 0 hours, 24 hours, 48 hours, and 72 hours post-wound (j). Mimic group: cells treated with miR-206 mimic. Lipo group: cells treated with lipofectamine. Data are expressed as mean ± SD. * means a statistical difference between experimental groups with $p < 0.05$. Scale bar: A and B 50; detail in A and B: 10; G: 200 µm.

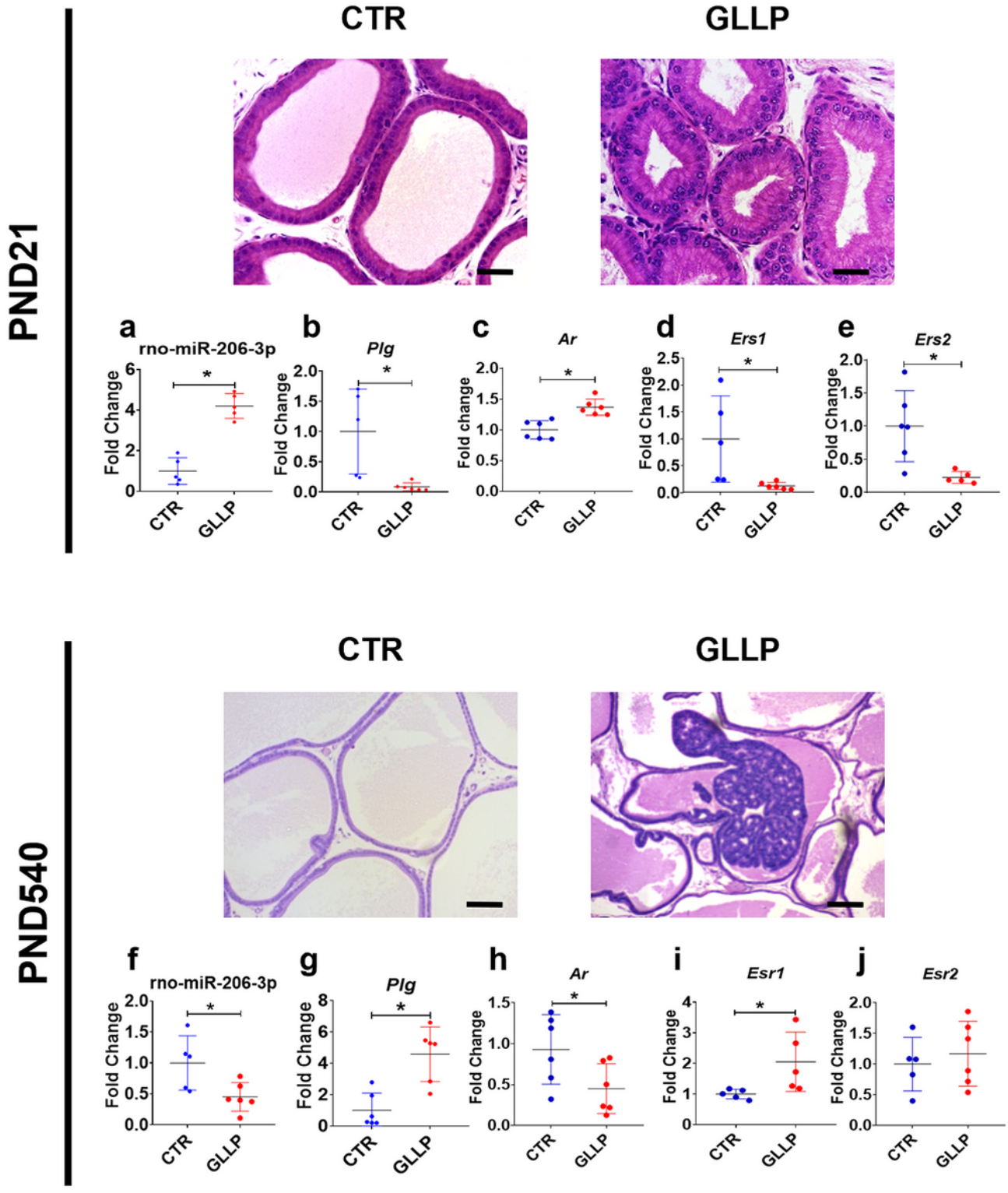

Figure 6

In vivo validation of *miR-206/Plg* network and steroids hormones receptors (*Ar*, *Esr1*, and *Esr2*) in the VP from the CTR and GLLP groups at PND 21 (a-e) and 540 (f-j). The results of *miR-206* (a, and f), *Plg* (b, and g), *Ar* (c, and h), *Esr1* (d, and i), and *Esr2* (e, and j) expression profiles were correlated with a delay in prostate growth in young rats from the GLLP group compared to the CTR group and with the

development of PCa in older rats submitted to maternal LPD. Data are expressed as mean ± SD. * means statistical differences between experimental groups with $p < 0.05$. Scale bar: 100 µm.

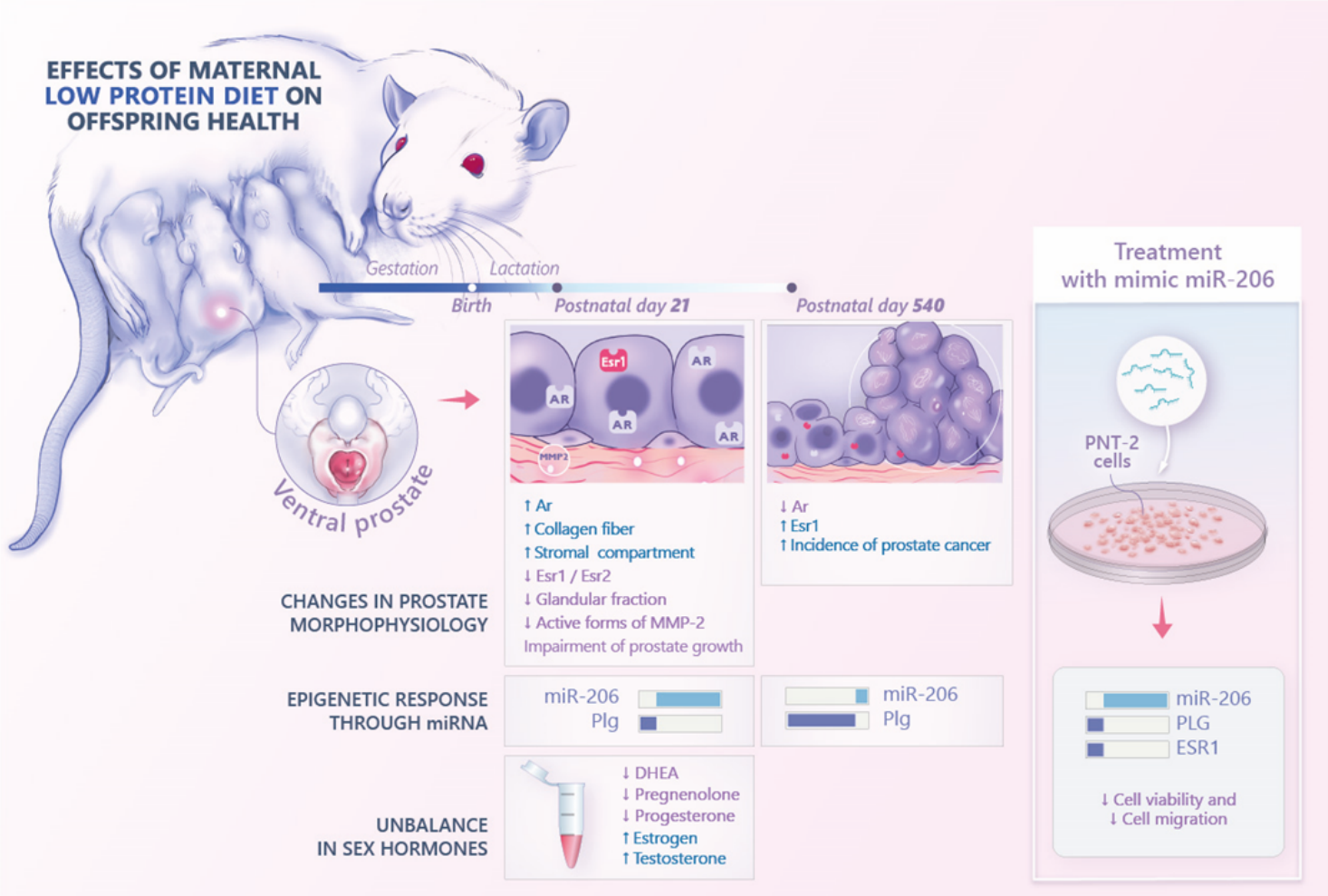

Figure 7

Overview of the main results. We associated maternal exposure to LPD with changes in the steroidogenesis process and impairment of prostate growth in young rats and increased incidence of carcinogenesis with aging. After looking at the RNA-seq data, the deregulation of the miR-206 network, together with changes in the expression profile of ERα (*ESR1*) were strongly described as a potential cancer driver involved in the developmental origin of prostate cancer in offspring rats exposed to maternal malnutrition.

Supplementary Files

This is a list of supplementary files associated with this preprint. Click to download.

- SupplementaryTableLuizPortela.xlsx